AGU PUBLICATIONS

JGR

Journal of Geophysical Research: Biogeosciences

RESEARCH ARTICLE
10.1002/2017JG004007

Key Points:
- DOM composition was vertically stratified with depth
- Microbial activity increased at the intermediate depth
- Our radiocarbon data suggested vertical/lateral advection with depth

Supporting Information:
- Supporting Information S1

Correspondence to:
M. M. Tfaily,
malak.tfaily@pnnl.gov

Citation:
Tfaily, M. M., Wilson, R. M., Cooper, W. T., Kostka, J. E., Hanson, P., & Chanton, J. P. (2018). Vertical stratification of peat pore water dissolved organic matter composition in a peat bog in northern Minnesota. *Journal of Geophysical Research: Biogeosciences*, *123*. https://doi.org/10.1002/2017JG004007

Received 26 JUN 2017
Accepted 22 JAN 2018
Accepted article online 29 JAN 2018

Vertical Stratification of Peat Pore Water Dissolved Organic Matter Composition in a Peat Bog in Northern Minnesota

Malak M. Tfaily[1], Rachel M. Wilson[2], William T. Cooper[3], Joel E. Kostka[4], Paul Hanson[5], and Jeffrey P. Chanton[2]

[1]Environmental Molecular Sciences Laboratory, Pacific Northwest National Laboratory, Richland, WA, USA, [2]Department of Earth Ocean and Atmospheric Science, Florida State University, Tallahassee, FL, USA, [3]Department of Chemistry and Biochemistry, Florida State University, Tallahassee, FL, USA, [4]School of Biology and School of Earth and Atmospheric Sciences, Georgia Institute of Technology, Atlanta, GA, USA, [5]Environmental Sciences Division and Climate Change Science Institute, Oak Ridge National Laboratory, Oak Ridge, TN, USA

Abstract We characterized dissolved organic matter (DOM) composition throughout the peat column at the Marcell S1 forested bog in northern Minnesota and tested the hypothesis that redox oscillations associated with cycles of wetting and drying at the surface of the fluctuating water table correlate with increased carbon, sulfur, and nitrogen turn over. We found significant vertical stratification of DOM molecular composition and excitation-emission matrix parallel factor analysis components within the peat column. In particular, the intermediate depth zone (~ 50 cm) was identified as a zone where maximum decomposition and turnover is taking place. Surface DOM was dominated by inputs from surface vegetation. The intermediate depth zone was an area of high organic matter reactivity and increased microbial activity with diagenetic formation of many unique compounds, among them polycyclic aromatic compounds that contain both nitrogen and sulfur heteroatoms. These compounds have been previously observed in coal-derived compounds and were assumed to be responsible for coal's biological activity. Biological processes triggered by redox oscillations taking place at the intermediate depth zone of the peat profile at the S1 bog are assumed to be responsible for the formation of these heteroatomic PACs in this system. Alternatively, these compounds could stem from black carbon and nitrogen derived from fires that have occurred at the site in the past. Surface and deep DOM exhibited more similar characteristics, compared to the intermediate depth zone, with the deep layer exhibiting greater input of microbially degraded organic matter than the surface suggesting that the entire peat profile consists of similar parent material at different degrees of decomposition and that lateral and vertical advection of pore water from the surface to the deeper horizons is responsible for such similarities. Our findings suggest that molecular composition of DOM in peatland pore water is dynamic and is a function of ecosystem activity, water table, redox oscillation, and pore water advection.

Plain Language Summary We found strong vertical stratification in dissolved organic matter molecular composition and optical properties within the peat column at the S1 bog. Surface samples were dominated by inputs from surface vegetation. The intermediate depth (~ 50 cm) was an area of high reactivity and increased microbial activity with diagenetic formation of many unique compounds such as polycyclic aromatic compounds (PACs) that contain both nitrogen and sulfur heteroatoms. These compounds were previously observed in coal-derived products and were assumed to be responsible for coal's biological activity. Biological processes taking place at the intermediate depth zone of the peat profile at the S1 bog are assumed to be responsible for the formation of these heteroatomic PACs in our system. Conversely, these compounds might stem from black carbon and nitrogen from potential fires that occurred at the site in the past.

1. Introduction

Boreal peatlands cover only 3% of the Earth's land surface, but their thick deposits store approximately one third of all soil carbon (C) (Frolking et al., 2011; Gorham, 1991; Limpens et al., 2008). Currently, peatlands represent a sink for carbon dioxide and source of atmospheric methane. Peatlands are classified as either ombrotrophic bogs that rely mostly on precipitation for water and nutrients or fens that are in contact

with mineral soil and ground water (Frolking et al., 2011). Boreal peatlands are extreme environments that challenge organisms by being cold, acidic, and poor in mineral nutrients. Vegetation is adapted to the harsh conditions and evolves in response to hydrology (Dise, 2009; Siegel et al., 1995; Siegel & Glaser, 1987). Bogs are dominated by *Sphagnum* mosses, while fen vegetation is dominated by vascular plants such as sedges (*Carex* spp.) whose root systems can reach into the anoxic peat layers. Carex and other typical peatland plants have adapted to the primarily anoxic environment by evolving an enlarged aerenchyma, intercellular spaces that form a gas conduit and allow transport of oxygen into roots (Armstrong et al., 2000).

While intensive research in the last decade has mostly examined upland systems draining into streams (Findlay et al., 2001; Huryn et al., 2001; Riley et al., 2003), northern peatlands are known to play an important role in the global carbon (C) cycle (Blodau et al., 2007). The coupling between C, nitrogen (N), and sulfur (S) cycling in peatlands is increasingly drawing attention owing to the possible ramifications for greenhouse gas emissions from such environments (Blodau et al., 2007). The presence of sulfate (originating from sulfur deposition) may decrease methane production through competition of anaerobic bacteria for substrates, such as acetate, alcohols, and hydrogen. Increases in N deposition can increase productivity and C assimilation and also release C if decomposition rates are accelerated through changes in N availability or species composition (Vanbreemen, 1995).

Dissolved organic matter (DOM) in peat pore waters is a critical driver in controlling a wide range of biogeochemical process in peatlands (Chanton et al., 2008; Corbett, Burdige et al., 2013; Corbett, Tfaily et al., 2013; Corbett et al., 2015). Water level and movement in peatlands has an important effect on C storage and flux. Thus, any change in the flux of DOM may result in a regional redistribution of terrestrial C (Holden, 2005). For example, decreased water table levels due to increased evapotranspiration with increasing temperatures will increase peat oxidation and possibly increase DOM fluxes. Global climate change (e.g., warming, draught, and nutrient deposition) is therefore likely to alter the carbon balance of peatland ecosystems (Dise, 2009) and hence DOM dynamics. There is, however, a high degree of uncertainty on the combined effects of climate warming and atmospheric CO_2 increase on DOM (Pendall et al., 2004). Climate change is also likely to drive changes in vegetation distribution (Parmesan & Hanley, 2015). These changes will impact the type of organic matter found in peatlands and their downstream catchments. Akagi and Zsolnay 2008 showed that the impact of vegetation changes will have a certain lag time due to the buffering effect of soils. Another changing parameter for peatlands may be an increase in primary productivity due to the increase in atmospheric CO_2 concentration (Freeman et al., 2004). This increase in primary productivity could then result in an increase in DOM exported from peatlands. To examine questions regarding the effects of a changing climate on DOM dynamics, we made measurements at a large-scale ecosystem manipulation (Spruce and Peatland Responses under Climatic and Environmental Change, SPRUCE) that has been implemented at a peat bog (S1 bog) at the Marcel Experimental Forest (MEF), Minnesota, USA. The landscape of the MEF is covered by forested uplands, peatlands, and lakes. Snow typically falls from November to April and the mean annual temperature is around 3.4°C (Griffiths & Sebestyen, 2016). The average peat thickness at the S1 bog is 2–3 m, whereas the water table levels fluctuates within the top 30 cm of peat and reaches its lowest values in late September and October due to prolonged periods of low precipitation levels (Parsekian et al., 2012; Sebestyen et al., 2011).

Peatlands are generally separated with depth into two main layers: the acrotelm and the catotelm. The acrotelm is usually oxic and dominated by living plants. The catotelm, on the other hand, is anoxic with organic matter stored as peat. The mesotelm was recently introduced (Clymo & Bryant, 2008) as a layer that represents a transition zone between the acrotelm and the catotelm. Redox oscillations due to fluctuating water table at this depth are hypothesized to increase carbon turn over in this layer. Recently, we (Tfaily et al., 2014) investigated the organic matter composition of the bulk peat soil at the S1 bog using Fourier transform infrared spectroscopy (FT-IR) and solid state nuclear magnetic resonance. In our previous Tfaily study, we revealed three zones within the peat column, with the intermediate depth zone (30–75 cm) to be the most reactive zone, and we proposed that oxygen levels and microbial community composition are the main drivers for the molecular variation in SOM composition. In the Tfaily study, however, we did not look at organic matter composition in the dissolved phase. Since the quality of peatland DOM, its composition and reactivity can be related in part its source, that is, soil organic matter, we therefore hypothesize that in the current study we will see a higher evidence of carbon, sulfur, and nitrogen turn over in the dissolved phase at the intermediate depth zone, facilitated by redox oscillations associated with cycles of wetting and drying at the surface of the water table. To test this hypothesis, we examined the molecular characteristics (i.e., bulk

composition and fluorescence properties) of DOM throughout the depth profile (5 cm–200 cm). Through the use of high-resolution mass spectrometry and excitation-emission matrix parallel factor analysis (EEM-PARAFAC) analysis, we highlight the importance of understanding processes that control DOM production and transformation with depth in peatlands.

2. Materials and Methods

2.1. Sampling and Site Location

The experimental site was the S1 bog within the Marcell Experimental Forest (MEF; N 47°30.476′; W93°27.162′), approximately 40 km north of Grand Rapids, Minnesota, USA. The MEF complex has been the subject of numerous studies over the last five decades in the areas of C sequestration, greenhouse gas emission, geomorphology, basic hydrology, geochemistry, and vegetation (Sebestyen et al., 2011). The bog surface is characterized by hummock and hollow microtopography with a relief of 10–30 cm between the tops of the hollows and the hummocks. For more detailed information about this site refer to Kolka (2011) and Tfaily et al. (2014). Extensive scientific investigations have been conducted at this site for several decades (Hanson et al., 2016; Nichols & Brown, 1980; Urban et al., 1989; Verry, 1981). The S1 bog is divided into three transects. The approximate dimension for each transect was as follows: T_1 = 88 m, T_2 = 112 m, and T_3 = 92 m. For this study, three experimental plot centers, within each transect, were chosen—Near (N), Mid (M), and Far (F)—from west to east across the bog. S1 bog vegetation consists of two dominant tree species, black spruce (*Picea mariana*) and larch (*Larix laricina*), with both hollow and hummock features. The bryophytes in hummocks consist mainly of *Sphagnum magellanicum*, while hollows are mainly colonized by *S. angustifolium*. Pore water samples for DOC, EEM-PARAFAC, and Fourier transform ion cyclotron resonance mass spectrometry (FT-ICR-MS) analysis were collected in July 2012 from three sites (mid, far, and near) along the T_3 transect (T_3M, T_3F, and T_1N) from depths ranging from 0 to 200 cm below the water table. The surface of the hollows was defined as 0 cm. A peristaltic pump with Teflon tubing was used to collect pore water from 1.25 cm diameter polyvinyl chloride piezometers at ~ 25 cm depth intervals, to a depth of 200 cm, below the water table, which was at the surface of the hollows in July 2012. Pore water samples were filtered through 0.7 μm glass-fiber filters (Whatman) immediately after collection and stored frozen until time of analysis.

2.2. DOC Analysis

The dissolved organic carbon (DOC) concentration of the different pore water samples collected from T3F, T3M, and T1N, reported as mM, was measured by high-temperature catalytic oxidation using a Shimadzu Total Organic Carbon analyzer equipped with a nondispersive infrared detector. Triplicate measurements were done for each sample, and the coefficient of variance was always $<$2%.

2.3. EEM-PARAFAC Analysis

Excitation-emission matrix spectroscopy (EEMS) fluorescence measurements were made at room temperature with a 10 mm path length cuvette using a Jobin Yvon SPEX Fluoromax-4 spectrometer with a Xenon lamp light source. Excitation wavelengths were scanned from 240 to 500 nm in 5 nm intervals, and emission was recorded between 290 and 600 nm in 2 nm increments. Highly concentrated DOM samples were diluted to AU $\leq$ 0.02 at 350 nm to prevent inner-filter effects (Andersson & Bro, 2000). The data integration time was 0.1 s, and data acquisition was carried out in signal/reference mode using a 5 nm band pass on both excitation and emission monochromators, normalizing the fluorescence emission signal with the excitation light intensity. FL toolbox 1.91 in MATLAB was used for postcollection data manipulation. Portions (±10–15 nm FW) of each scan centered on the respective scatter peak were excised to eliminate Rayleigh and Raman scattering peaks. Data were then normalized to a daily-determined water Raman intensity (350ex/397em, 5 nm band pass) following removal of scatter peaks and converted to Raman-normalized quinine sulfate equivalents in ppb. To account for dilution the scatter-corrected fluorescence of the diluent, Milli-Q water was subtracted and the resultant fluorescence values were multiplied by the dilution factor to obtain the intensity for the original, undiluted sample. Positions and intensities (Ex/Em max values) of individual fluorescent peaks were determined to gain information on the composition and source of the DOM. Repeat analysis of DOM showed that the fluorescence intensity of the different components of the excitation-emission matrix (EEM) had a relative standard deviation of $<$5%. Sample transfer and storage (e.g., freezing) may contribute to somewhat higher uncertainties to these measurements.

PARAFAC was used to statistically decompose EEMS into fluorescent groups/components (Ohno & Bro, 2006; Stedmon et al., 2003). Here PARAFAC modeling was applied by fitting the EEMS to a five-component PARAFAC model (Tfaily et al., 2015), which was established for northern Minnesota peatlands. The analysis was carried out in MATLAB 7.0.4 (Mathworks, Natick, MA) with the DOM Fluor toolbox (Stedmon & Bro, 2008). No obvious residues were found after fitting the pore water EEMS to the model, indicating it was applicable. This approach can facilitate the comparison of pore waters from different peatlands. The five components (referred to as C1 through C5) were assigned as four humic like and one protein like (Table S1 in the supporting information) based on the comparison of spectral characteristics with FT-ICR data and previous studies (for more detailed information of the identity of each component please refer to Tfaily et al., 2015). C1 is a mixture of terrestrial humic-like peaks A and C, whereas C2 is microbially degraded humic-like material. C3 was identified as a microbially produced humic-like component. C4 has been associated with either ubiquitous humic-like organic matter that is of higher molecular weight and more aromatic, and finally, the spectral pattern of C5 resembled those of tryptophan-like fluorophores: free amino acids or amino acids bound in protein molecular structures.

The ratio of peak C fluorescence to absorbance at 340 nm has been used as an indicator of DOM molecular weight (MW), with this ratio increasing as a function of decreasing DOM MW. The peak C emission wavelength is characteristic of unsaturation, increasing with an increase in the number of highly substituted aromatic nuclei and conjugated systems (Senesi, 1990). When these two parameters are combined, samples differing in unsaturation and molecular weight can be clearly distinguished.

2.4. FT-ICR MS Measurements

High-resolution mass spectra of selective pore water DOM samples (in this case T3M) were collected on a custom-built FT-ICR mass spectrometer with 9.4 Tesla superconducting magnet located at the National High Magnetic Field Laboratory. EEM-PARAFAC data showed that the DOM composition is significantly different with depth rather than across the three sites. The use of FT-ICR-MS to investigate the composition of organic matter has been described in detail in Tfaily et al. (2011, 2012, 2013). A solution containing the DOM sample and methanol was injected into the instrument at a final concentration of 500 mg C/L. Samples were then introduced to an electrospray ionization (ESI) source through a syringe pump at a flow rate of 0.5 lL/min that was equipped with a 50 lm i.d. fused silica tube (Chowdhury et al., 1990). Two hundred individual scans were summed, and the average resolving power (m/Δm 50%) was >700,000 at 451 Da. All observed ions were singly charged as confirmed by the 1.0034 Da spacing found between isotopic forms of the same molecule (i.e., between $^{12}C_n$ and $^{12}C_{n-1}$–$^{13}C_1$). Two internal series of DOM homologous series separated by 14 Da (–CH_2 groups) were used to calibrate spectra internally, and the mass accuracy was calculated to be <1 ppm for singly charged ions ranging across the mass spectral distribution (*m/z* 300–900). National High Magnetic Field Laboratory MS software was used to calculate all possible molecular formulas within a ± 1 ppm error taking into consideration the presence of C, H, O, N, and S and excluding other elements. The data were visualized by the van Krevelen diagram, one of the most common ways for visualizing these large data sets. The van Krevelen diagram plots the elemental ratios of oxygen to carbon (O/C) and hydrogen to carbon (H/C) in each formula on the *x* and *y* axes, respectively, and is utilized to assist in clustering molecules according to their functional group compositions. The unique O/C and H/C ratios for each formula align and fall within areas that are representative of specific types of molecules. The following ranges were used in this study: lipids ($0 < O{:}C \leq 0.3$, $1.5 \leq H{:}C \leq 2.5$), unsaturated hydrocarbons ($0 \leq O{:}C \leq 0.125$, $0.8 \leq H{:}C \leq 2.5$), proteins ($0.3 < O{:}C \leq 0.55$, $1.5 \leq H{:}C \leq 2.3$), amino sugars ($0.55 < O{:}C \leq 0.7$, $1.5 \leq H{:}C \leq 2.2$), carbohydrates ($0.7 < O{:}C \leq 1.5$, $1.5 \leq H{:}C \leq 2.5$), lignin ($0.125 < O{:}C \leq 0.65$, $0.8 \leq H{:}C < 1.5$), tannins ($0.65 < O{:}C \leq 1.1$, $0.8 \leq H{:}C < 1.5$), and condensed hydrocarbons ($0 \leq O{:}C \leq 0.95$, $0.2 \leq H{:}C \leq 0.8$). This visualization tool not only identifies what types of compounds are present in the sample but also highlights variations between samples by overlaying numerous plots.

3. Results

3.1. DOC Analysis

DOC concentrations (Figure S1) of the pore water collected from the three sites (T_1N, T_3M, and T_3F) ranged between 3 and 7 mM (36–84 Mg C L^{-1}). DOC values dropped slightly below the surface to increase again

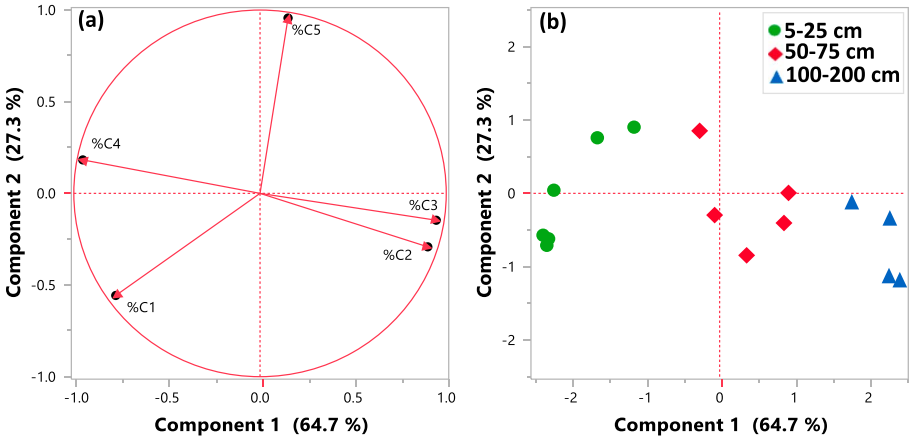

Figure 1. Graphical representation of principle component analysis of the excitation-emission matrix-parallel factor analysis (PARAFAC) relative abundances for all samples collected from the S1 bog from three transects. (a) Loadings plot for the different PARAFAC components pore water parameters and (b) score plot for pore water samples grouped using a cluster analysis and classified on the basis of location (site), depth, and different PARAFAC components. The terrestrial (C1 and C4) and microbial/protein (C3–C5) components have dissimilar distributions along principal component 1, suggesting that the dissolved organic matter source controls principal component 1.

and reach a maximum at around 50 cm consistent with increased peat decomposition at that depth (Tfaily et al., 2014). Below the intermediate depth zone, the DOC concentrations drop signifcantly.

3.2. EEM-PARAFAC Analysis

The relative abundance of all the EEM-PARAFAC components (Table S1) C1 through C4 was significantly different with depth (Figure S3), except for C5. The same data were used for Principle Component Analysis (PCA). The resulting loadings and scores are shown in Figures 1a and 1b, respectively. Principal Component 1 (PC1) accounted for 74.4%, and Principal Component (PC2) accounted for another 21.3% of the variability. As illustrated in the loading plot of PCA (Figure 1a), the five PARAFAC components are distributed along PC1 such that the relative abundance of humic-like terrestrial C4 and C1 (Tfaily et al., 2015) correlates most negatively with PC1, and the relative abundance of humic microbial-like C3, C2, and protein-like C5 (Tfaily et al., 2015) is positively correlated with PC1. The terrestrial and microbial/protein components have dissimilar distributions along PC1, suggesting that the DOM source controls PC1. Along PC2, the loadings of components are distributed with C1, C2, and C3 as the most negative and C4 and C5 the most positive. C4 is more abundant in surface samples and decreases with depth (Figure 2), whereas C3 is more abundant in intermediate and deep samples and increase with depth.

Surface samples from the S1 bog sites were separated from the intermediate depth samples that in turn were separated from the deep samples (Figure 1b). The score plot (Figure 1b) shows that the source variation, represented by PC1, is an important driver of DOM character in the S1 bog (T_3M, T_3F, and T_1N) across the three depth zones. Less variation was observed in DOM composition across the three sites in S1 bog (T_3F versus T_3M versus T_1N) across PC2.

PC1 scores negatively correlate with humic-like terrestrial fluorescence C1 ($p < 0.01$, $r = 0.9$) and humic-like ubiquitous C4 ($p < 0.01$, $r = 0.827$), two indicators of DOM input from surface vegetation. The most negative PC1 scores are found in surface samples from T1N, T3F, and T3M. PC1 scores positively with protein-like fluorescence C5 ($p < 0.01$, $r = 0.07$), humic-like microbially degraded C2 ($p < 0.01$, $r = 0.95$), and humic-like microbially produced C3 ($p < 0.01$, $r = 0.9$). The most positive PC1 score was observed in deep pore water samples, followed by intermediate depth pore water samples that suggest evidence of microbial utilization of pore water DOM deeper in the peat column. Moreover, both microbially degraded humic-like component C2 and microbially produced humic-like component C3, which both increased with depth at the S1 bog (Figure 2), were positively correlated ($r^2 = 0.71$) to each other and negatively correlated to ubiquitous high MW humic-like component C4 ($r^2_{C2} = 0.67$ and $r^2_{C3} = 0.76$).

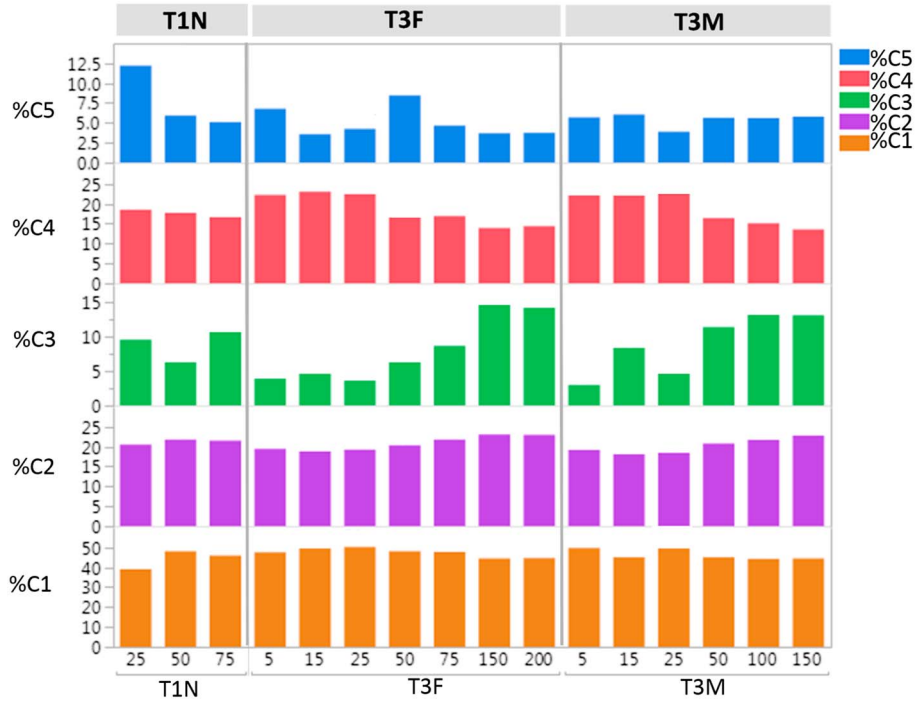

Figure 2. Relative contributions of the five components identified by the parallel factor analysis model for all the samples from three sites (T3F, T3M, and T1N). Depth of samples increases for each site from left to right. Refer to Tfaily et al., 2015 for further description of the components; briefly, component 1 represents relatively intact humic substances, component 2 appears to be microbially altered humic material, component 3 has been identified as humic like and derived specifically from lignin, component 4 has been associated with either ubiquitous humic-like organic matter that is composed of high molecular weight and aromatic organic compounds and/ or terrestrial reduced quinine-like compounds, and component 5 has been identified as "protein like."

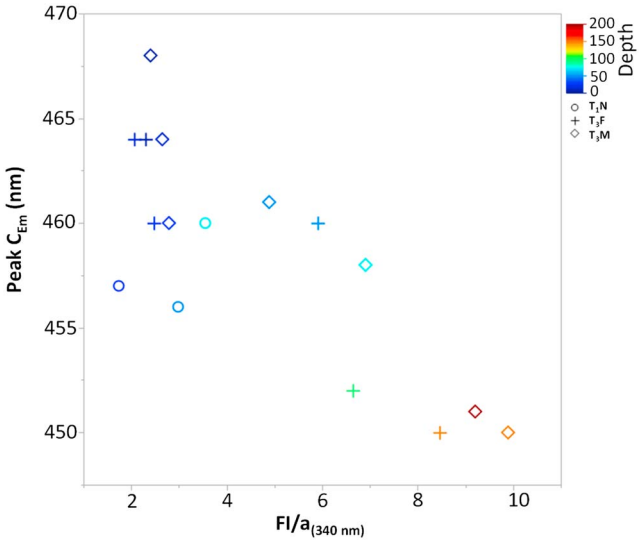

Figure 3. Fluorescence: absorbance ratio (FI/a (340 nm) versus peak C emission wavelength for T3M, T3F, and T1N samples. FI/a (340 nm) decreases with increasing molecular weight (MW), while peak C emission wavelength increases as conjugation and aromaticity increase. Surface samples are characterized by high MW dissolved organic matter and high aromaticity compared to the deep samples that are characterized by low MW dissolved organic matter and low aromaticity. Depth is reported in centimeters.

A plot of peak C emission wavelength versus the fluorescence/absorbance ratio (Figure 3), yielded three distinct groups: surface DOM samples with low fluorescence/absorbance ratios and high peak C emission wavelengths, especially for surface samples. Intermediate depth DOM samples exhibit relatively high low fluorescence/absorbance ratios and higher peak C emission wavelengths. Deep DOM is characterized with high fluorescence/absorbance ratios. These differences indicate that surface samples are characterized by high MW DOM and high aromaticity compared to the deep samples that are characterized by low MW DOM and low aromaticity.

3.3. FT-ICR-MS Analysis

Figure 4 shows the negative ion mass spectra of the solid phase extraction (SPE)-extracted pore water samples from four depths. The DOM mass spectra consist of a multitude of peaks spanning the *m/z* range of 200–1,000, and complexity is apparent from the detection of up to 17 peaks per nominal mass at nearly every mass throughout that range. From the expanded insets of Figures 4a–4d, one can note that the peaks are singly charged due to the observation of the isotopic peaks at 1.00335 *m/z* units (the mass of a neutron) higher than the parent peak. Figures 4e–4h show expanded regions at nominal 532 *m/z*. The striking difference is that middepth samples (50, 75 cm) are more

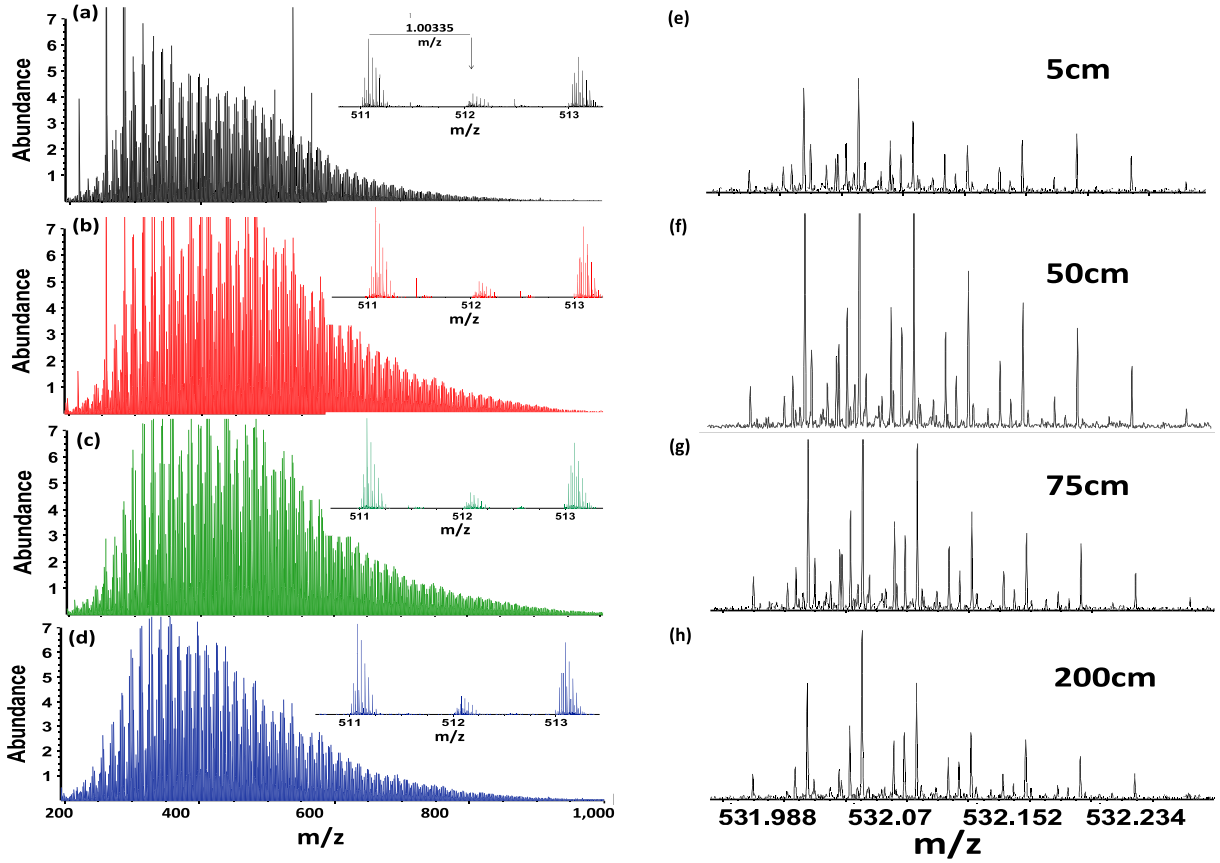

Figure 4. Negative ion mass spectrum (*m/z* 200–100) of pore water dissolved organic matter from T3M at (a) 5 cm, (b) 50 cm, (c) 75 cm, and (d) 200 cm. Expanded region of each spectra that include mass 531.988–532.234 that highlights the complexity at each nominal mass: (e) 5 cm, (f) 50 cm, (g) 75 cm, and (h) 200 cm.

complex than surface and deep DOM samples, which in turn appear similar to each other. In particular, intermediate depth samples have more peaks with low mass defect (i.e., exact masses near the nominal mass) compared to surface and/or deep DOM samples. This trend is observed at more than one nominal mass throughout the whole *m/z* range, in particular for compounds with molecular weight $>$ 500 *m/z*. DOM in the surface most and deepest samples include fewer compounds characterized by high molecular weight and low mass defect than DOM in the middepths. It should be remembered that the FT-ICR-MS is indicative of the number of specific or unique compounds and is not quantitative with respect to the concentrations of those specific compounds. Thus, Figure 3 indicates that overall, molecular weight decreases with depth, while in the FT-ICR-MS data there are more unique high molecular weight compounds at the middepths. For this reason, pairing EEM-PARAFAC measurements and FT-ICR-MS is useful.

To better visualize the changes in the molecular composition in DOM with depth, we compared the composition of DOM from each two adjacent depths (i.e., 5 cm versus 50 cm, 50 cm versus 75 cm, and 75 cm versus 200 cm) and reported the unique peaks present at each depth on a van Krevelen diagram (Figures 5a, 5c, and 5e). Here "unique" refers to formulas identified in one but not both of the depths compared. For example, a formula unique to the 5 cm depth implies that it is lost/degraded somewhere between 5 and 50 cm, while a formula unique to the 50 cm depth implies that it was formed somewhere between 5 and 50 cm. We additionally took the unique peaks from each comparison and calculated the percent abundance of the different compound classes and plotted that as a pie chart, so that the pie charts represent the abundances (magnitude weighted) of different compound classes present uniquely in a sample upon comparing with a sample from an adjacent depth (Figures 5b, 5d, and 5f). DOM in the surface sample (5 cm) appeared more rich in lipid-like ($0 < O{:}C \leq 0.3$, $1.5 \leq H{:}C \leq 2.5$) and protein-like ($0.3 < O{:}C \leq 0.55$, $1.5 \leq H{:}C \leq 2.3$) compounds that are presumably of higher plant origin and released directly by the surface vegetation (Figures 5a and 5b). Conversely, DOM from 50 cm shows a large increase in the abundance of condensed aromatics (i.e.,

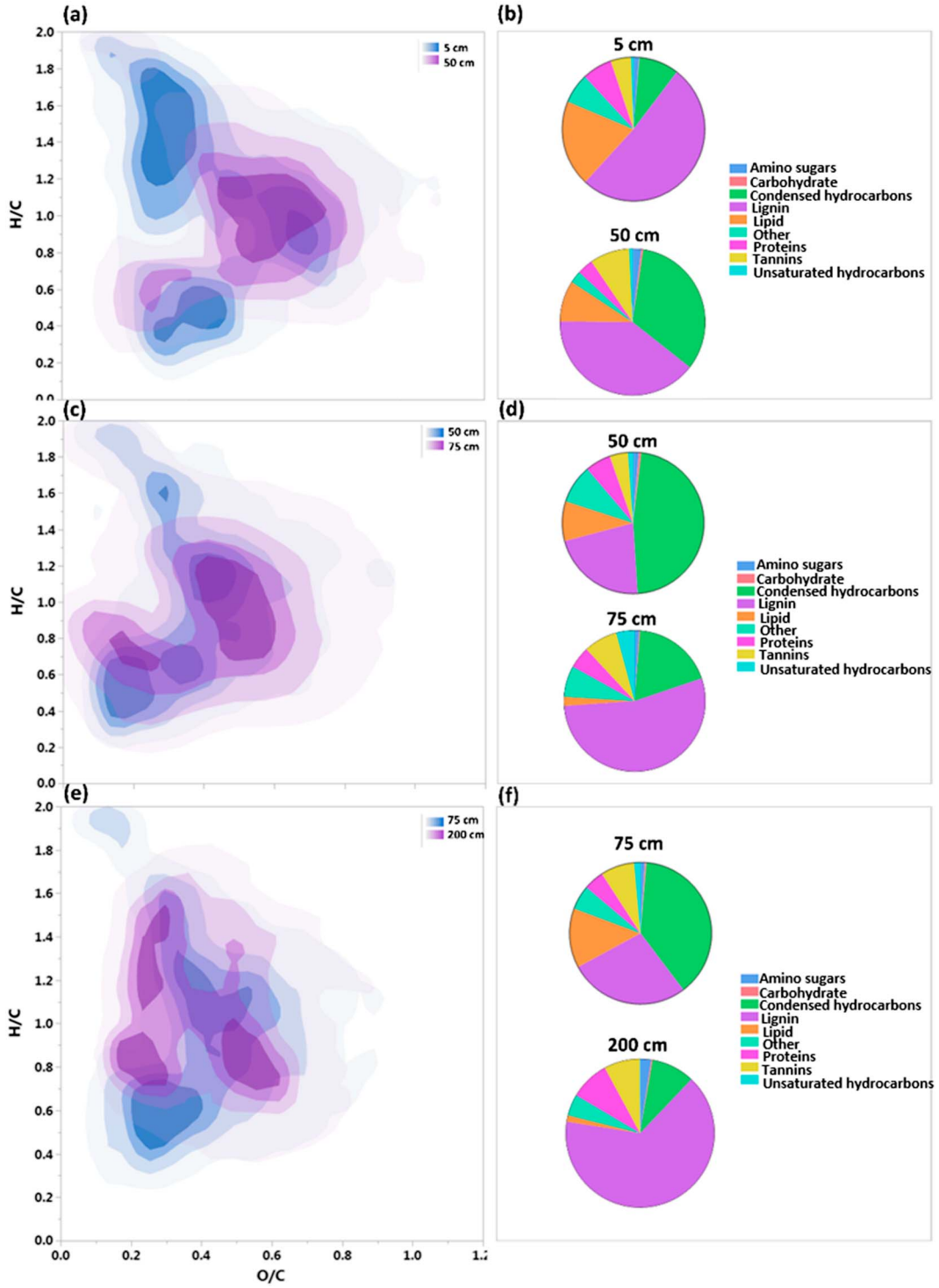

Figure 5. van Krevelen diagrams (a, c, e) and pie charts (b, d, f) generated from Fourier transform ion cyclotron resonance mass spectrometry data of pore water dissolved organic matter (DOM). In this graph we compare the composition of DOM from each two adjacent depths to follow DOM decomposition dynamics and reported the unique peaks present at each depth on a van Krevelen diagram. We additionally took the unique peaks from each comparison and calculated the percent abundance of the different compound classes and plotted that as a pie chart so that the pie charts represent the abundances (magnitude weighted) of different compound classes present uniquely in a sample upon comparing with a sample from an adjacent depth. (a and b) Comparison of DOM in the 5 and 50 cm zone, (c and d) comparison of DOM in the 50 and 75 cm zone, and (e and f) comparison of DOM in the 75–200 cm.

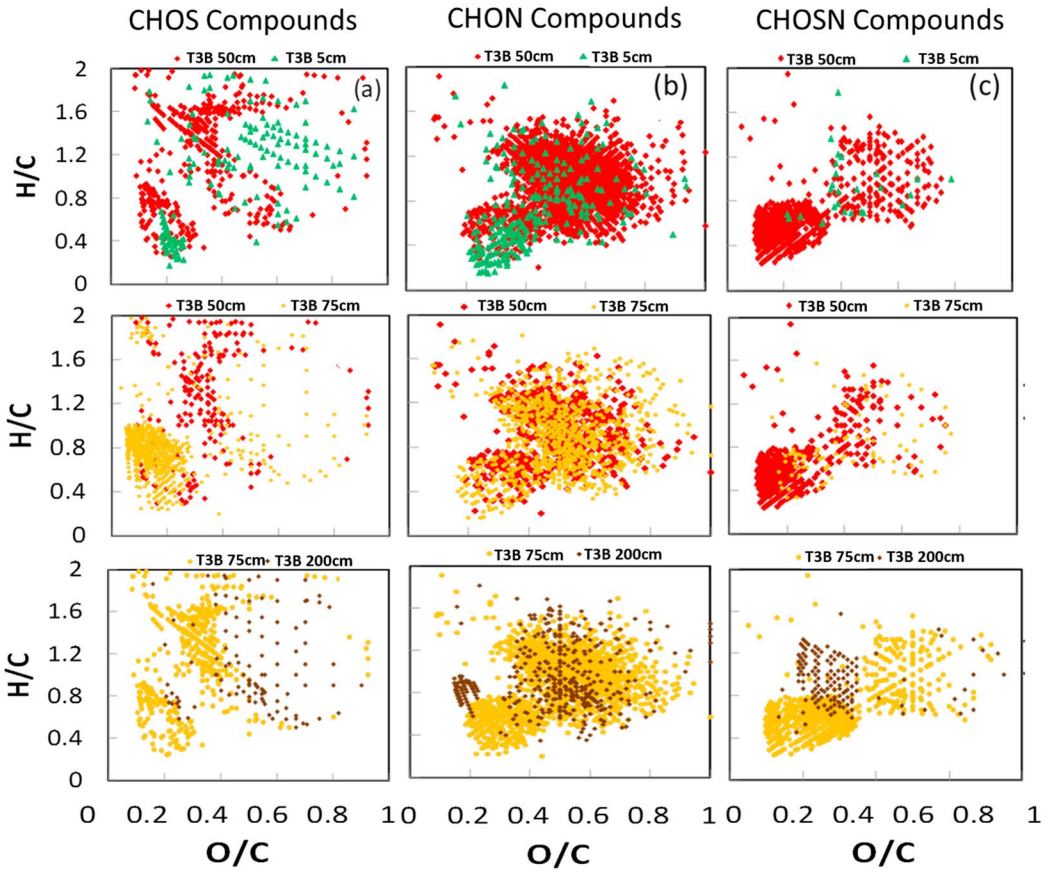

Figure 6. van Krevelen diagrams of the formulas containing (a) sulfur, (b) nitrogen, and (c) NS that are unique to a particular depth after comparison with an adjacent depth. (top row) Comparison between 5 and 50 cm. (middle row) Comparison between 50 and 75 cm. (bottom row) Comparison between 75 and 200 cm. CHOS = carbon, hydrogen, oxygen, and sulfur; CHON = carbon, hydrogen, oxygen, and nitrogen; CHOSN = carbon, hydrogen, oxygen, sulfur, and nitrogen.

compounds with multiple fused aromatic rings) ($0 \leq$ O:C ≤ 0.95, $0.2 \leq$ H:C ≤ 0.8) relative to the 5 cm sample and a corresponding decrease in the abundance of protein-like (component 5) and lipid-like compounds (Figures 5a and 5b).

When comparing the DOM in the 50 and 75 cm horizons (Figures 5c and 5d), less condensed aromatic compounds were observed at 75 cm relative to 50 cm, and there was an increase in the abundance of lignin-like compounds (compounds with single aromatic rings; $0.125 <$ O:C ≤ 0.65, $0.8 \leq$ H:C < 1.5). The reduction of condensed aromatic compounds is accompanied by an increase in aliphatic compounds (unsaturated hydrocarbons). The decrease in condensed aromatic compounds and the accumulation of lignin-residue compounds continues with depth when DOM at 75 cm and 200 cm are compared (Figure 5e). Interestingly, the deep sample (200 cm) has a similar composition to surface samples (5 cm) but with more lignin-like compounds found in place of lipid-like compounds.

3.3.1. S-Containing Compounds

To better follow N and S dynamics along the peat profile, we compared the composition of DOM from each two adjacent depths (i.e., 5 cm versus 50 cm, 50 cm versus 75 cm, and 75 cm versus 200 cm) and reported the S and/or N unique peaks present at each depth on a van Krevelen diagram (Figure 6). Here unique refers to formulas identified in one but not both of the depths compared. For example, a formula unique to the 5 cm depth implies that it is lost/degraded somewhere between 5 and 50 cm, while a formula unique to the 50 cm depth implies that it was formed somewhere between 5 and 50 cm. We additionally took the unique peaks from each comparison and calculated the percent abundance of the different class types and plotted that as a pie chart so that the pie charts represent the abundances (magnitude weighted) of different classes present uniquely in a sample upon comparing with a sample from an adjacent depth (Figure 7).

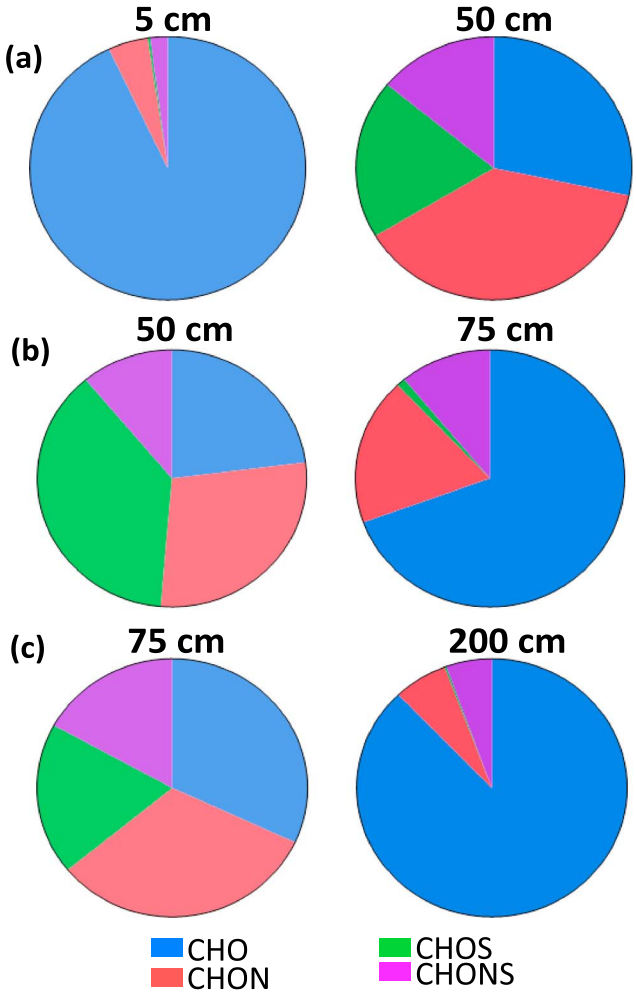

Figure 7. Pie charts of the percent relative abundances of class types as revealed by Fourier transform ion cyclotron resonance mass spectrometry that are present uniquely in sample upon comparing with a sample from an adjacent depth: (a) comparison between 5 and 50 cm, (b) comparison between 50 and 75 cm, and (c) comparison between 75 and 200 cm. Note that unique compounds containing both N and S form at 50 cm, but no unique CHONS compounds were generated below that depth. CHONS compounds in the right column at 75 cm are residual compounds produced at 50 cm that were steadily consumed below 50 cm. CHO = carbon, hydrogen, and oxygen; CHOS = carbon, hydrogen, oxygen, and sulfur; CHON = carbon, hydrogen, oxygen, and nitrogen; CHONS = carbon, hydrogen, oxygen, nitrogen, and sulfur.

An increase in the percent of S-containing organic compounds (only carbon, hydrogen, oxygen, and sulfur (CHOS) compounds) at the 50 cm horizon was observed, compared to the 5 cm horizon (Figures 6a and 7a). Upon comparing between the composition of DOM at 50 and at 75 cm (Figures 6a and 7b), mineralization of the organic S compounds that was produced at the 50 cm horizon and incorporation of N into CHOS compounds (Figures 6a and 7b) were observed. At the intermediate depth, the decomposition of peat slows (Tfaily et al., 2014), and hence, microbial organisms may utilize organosulfur compounds that are present or produced at the 50 cm horizon. This mineralization of S compounds was accompanied by production of high MW organic sulfur (Figures 6a and 7b). Below the 75 cm horizon, there is clearly a shift from an environment where sulfate cycling and mineralization are occurring to an environment where mineralization of S containing compounds in the pore water occurs and where peat decomposition reaches a minimum (Figures 6a and 7c). Mineralization of organic compounds at the 75 cm horizon was accompanied by production of short chain or low MW organic molecules (Novak et al., 2000).

3.3.2. N-Containing Compounds

DOM at the 5 cm horizon contained unique nitrogen compounds (carbon, hydrogen, oxygen, and nitrogen, CHON) (Figure 7b) characterized primarily by low O/C and H/C ratios (Figure 6b), compared to the 50 cm horizon. These compounds disappear in 50 cm horizon with the appearance of two clusters of nitrogen-containing compounds and a group of CHONS compounds which will be discussed below (Figure 6b). The first set of 50 cm-appearing compounds is characterized by low O/C and an H/C ratio between 0.4 and 0.8. The second set of 50 cm-appearing compounds is characterized by higher O/C and H/C ranging between 0.4 and 1.6. Upon comparing DOM composition at 50 and 75 cm (Figures 6b and 7b), we observe the formation of CHON compounds in the same van Krevelen space as the 50 cm samples that were consumed. Upon comparing DOM at 75 and 200 cm (Figures 6b and 7c) horizon, a consumption of CHON compounds was observed accompanied by a slight production of new CHON compounds.

3.3.3. S,N-Containing Compounds

DOM in the 5 cm horizon does not have many unique carbon, hydrogen, oxygen, nitrogen, and sulfur (CHONS) compounds (Figures 6c and 7a), but their abundance increases markedly at the 50 cm horizon. Again, two groups of CHONS compounds were observed at that horizon that is absent at the 5 cm horizon: Group 1, characterized by high O/C and H/C ratios, and group 2 characterized by very low O/C and H/C ratios. CHONS compounds, formed or produced at the 50 cm horizon, were consumed at the 75 cm horizon (Figures 6c and 7b). Upon comparing DOM at 75 and 200 cm horizon, less CHONS compounds were observed between these depths (Figures 6c and 7c).

4. Discussion

4.1. DOC Analysis

Vertical stratification of DOC concentration within the peat column at the S1 bog was observed across the three different zones: acrotelm, mesotelm, and catotelm. The decrease in the pore water DOC below 50 cm was not consistent with the slow decomposition (and increased humification) observed in the solid peat with depth at the same site (Tfaily et al., 2014), consistent with the idea that microbial communites at

the S1 bog are preferentially utlizing DOC deep in the peat column. These observations support radiocarbon measurements in Tfaily et al. (2014) and Wilson et al. (2016), where radiocarbon signatures of microbial respiration products in deeper catotelm static zone resembled those of DOC rather than solid peat, indicating that carbon derived from recent photosynthesis and peat in upper layer fuels the bulk of the decomposition at depth, even in the catotelm. Since the bulk of the respiration products (dissolved CO_2 and CH_4) within the peat column resemble the DOC, and that DOC at depth has a surface derived ^{14}C signature (Tfaily et al., 2014; Wilson et al., 2016), the rate of microbial respiration within the peat column at S1 bog is suggested to be greater than the rate of solid phase peat decomposition (Tfaily et al., 2014). Lateral and vertical advection are responsible for the renewal of DOM at depth.

4.2. EEM-PARAFAC Analysis

PCA data further revealed vertical stratification in PARAFAC components at the S1 bog. PC1 correlated positively with C5 (protein like), C2 (humic like microbially degraded), and C3 (humic like microbially produced). The most positive PC1 score was observed in deep pore water samples, followed by intermediate depth pore water samples that suggest evidence of microbial utilization of pore water DOM deeper in the peat column. The decrease in the ubiquitous high MW humic-like component C4 with depth and the increase in C2 and C3 are in contrast to observations from a previous study in another northern peatland (Tfaily et al., 2015) where C3 was negatively correlated with C1, and C4 was relatively refractory. These data suggest that at the S1 bog, high molecular weight highly aromatic C4 appears to be more bioavailable for microbial communities than the C1 component and that DOM decomposition dynamics vary across different peatland sites. The increase in C3 and C2 and the decrease in C4 begin in the intermediate depth zone and continue to increase (C3 and C2) or decrease (C4) with depth (Figure 2), reflecting microbial utilization of pore water DOM at the S1 bog in the catotelm. The gradual increase in the microbially produced and degraded C3 and C2, respectively, with depth in this current study may reflect accumulation of these components with depth and/or production of more DOM at each horizon within the peat column in parallel with consumption of C4 compounds. The low DOC concentration values at depth (Figure S1) may suggest that consumption rates are higher than production rates. DOC-normalized fluorescence intensity plots of peaks A, (C + M) and T peaks, corresponding to components C1, C2 + C3, and C5 (Figure S2) are consistent with these observations, furthermore suggesting that C4 is the bioavailable component in this peatland. PC2 is almost exclusively driven by depth ($p < 0.01$, $r = 0.87$) with deeper samples having the most negative scores, followed by intermediate depths with scores around 0 and then surface depths with positive scores.

The low fluorescence/absorbance ratios and high peak C emission wavelengths observed for surface samples suggest that organic matter leached from plants is of high MW and relatively high conjugation. The increase in fluorescence/absorbance ratio at the intermediate depth is indicative of decomposition and increase in the abundance of low MW compounds. Deep DOM is characterized with high fluorescence/absorbance ratios indicating lower molecular weight and low peak C emission wavelengths hence reflecting less conjugation and the highly decomposed state of these samples and abundance of microbially produced DOM, consistent with the PARAFAC data (decrease in C4 component).

4.3. FT-ICR-MS Analysis

The higher abundances of lipid-like, protein-like, and amino sugars, and C4 in the surface DOM compared to DOM at 50 cm (Figures 2 and 5e) are consistent with the biodegradability of leachates from surface vegetation being readily utilized by microbial organisms in the upper 50 cm of the peat. At 50 cm, the intermediate depth zone, microbial activity, and SOM decomposition reaches a maximum, resulting in the production and leaching of a wide range of condensed aromatic compounds. These data are also consistent with the PARAFAC data that showed a correlation between samples at the intermediate depth and percent abundance of C2 and C3 (microbially produced and degraded DOM). Below the intermediate depth the abundance of condensed aromatics decreases, again suggesting that these compounds are somewhat bioavailable. The deep DOM sample has similar characteristics to the surface sample and is rich in lignin-like residue that are of plant terrestrial origin. These compounds were not utilized at the intermediate depth and thus were advected and accumulated in the deeper depths. At the intermediate depth zone, DOM composition appeared to be the most chemically compared to the other two zones (Figures 5 and 6) where the relative proportions of compounds containing elements other than C, H, and O are depicted. The compounds with only CHO decrease in magnitude with depth especially at the middepth horizon, while compounds

containing nitrogen and sulfur functionalities increase in magnitude and become the major contributors to the peak magnitude. At the 200 cm horizon, compounds with only CHO become the major contributors to the peak magnitude again (Figure 6).

Surface and deep DOM exhibited relatively similar characteristics, with the deep layer having a higher input of microbially degraded organic matter than the surface suggesting that DOM in the entire peat profile is derived from similar parent material and presents in different degrees of decomposition at different depths. Lateral and vertical advection of pore water from the surface to the deeper horizons is responsible for this distribution. However, the intermediate depths in the profile experience increased decomposition compared to the surface and deep horizons and the most diverse compositional array of DOM compounds. We attribute this to redox oscillations at the intermediate depth zones that facilitated changes in the water table levels with time and with seasons.

4.3.1. S-Containing Compounds

The increase in the percent of S-containing organic compounds (only CHOS compounds) at the 50 cm, compared to 5 cm (Figures 6a and 7), may be due to two processes that rapidly turn over S. The intermediate depth zone (50–75 cm) is characterized by intensive peat decomposition compared to the upper and underlying layers (Tfaily et al., 2014). During mineralization of peat (either biochemically through enzymatic hydrolysis or biologically through microorganisms), C-bonded S and ester sulfates are mineralized and result in dissolved free SO_2^{4-}. This explanation is supported by the presence of sulfite reductase genes that are affiliated with the Syntrophobacteraceae in this peat soil at that particular depth, as determined by Lin, Tfaily, Green, et al. (2014). Syntrophobacteraceae are known to have roles in both syntrophic fermentation and in respiring sulfate. With liberation of sulfate from the organic matter, sulfate-reducing bacteria oxidize organic matter and produce hydrogen sulfide. Part of the hydrogen sulfide could be reincorporated into organic matter that could leach back into pore water and be detected by FT-ICR-MS, and part could be oxidized again into sulfate. This cycling must occur rapidly since sulfate concentrations in pore water were below detection limit (data not shown) (Lovley & Klug, 1986). The oxidation of hydrogen sulfide released from the anaerobic peat is possible because microbial community composition showed that genes associated with sulfur oxidation were observed in abundance at 50 cm depth based on metagenomic analysis (Lin, Tfaily, Steinweg, et al., 2014; Lin, Tfaily, Green, et al., 2014).

Similarly, upon comparing between the composition of DOM at 50 and at 75 cm, we observed mineralization of the organic S compounds that were produced at the 50 cm horizon and/or incorporation of N into CHOS compounds (Figures 6a and 7b) that will be discussed below. Interestingly, at the intermediate depth (50–75 cm), the decomposition of peat slows (Tfaily et al., 2014), and hence, microbial organisms may utilize organo-sulfur compounds that are present or produced at the 50 cm horizon. This mineralization of S compounds was accompanied by production of high MW organic sulfur compounds either by direct incorporation of sulfate into organic matter to form sulfur esters or by H_2S incorporation into organic matter. Below the 75 cm horizon (Figures 6a and 7c), there is clearly a shift from an environment where sulfate cycling and mineralization are occurring to an environment where mineralization of S containing compounds in the pore water occurs and where peat decomposition reaches a minimum. Mineralization of organic compounds at the intermediate depth was accompanied by production of short chain or low MW organic molecules (Novak et al., 2000).

4.3.2. N-Containing Compounds

Some of the nitrogen found in the peat soil originated due to N_2 fixation as N_2 fixing bacteria were found to be abundant above 75 cm in the peat at S1 bog, with lower abundance in the deeper peat (Figures 6b and 7), (Lin, Tfaily, Steinweg, et al., 2014; Lin, Tfaily, Green, et al., 2014), consistent with the distribution of ammonium that increased with depth. At the intermediate depth zone of 50 cm, FT-ICR-MS data suggested the greatest incorporation of N into a broader array of dissolved organic compounds. These processes are consistent with the soil organic matter analysis that showed a marked decrease in C/N ratios at the intermediate depth and a threefold increase in soil nitrogen, suggesting N immobilization (Tfaily et al., 2014). At this depth (50 cm) FT-ICR-MS analysis of DOM reveals formation of N-containing compounds that could arise from two sources: (1) incorporation of N into organic matter and (2) reaction of decomposed organic matter with small molecular weight N-containing compounds. Moreover, inorganic N reacts chemically with organic matter to form stable organic N complexes that would lower the concentration of inorganic N. Below the active zone ($>$ 50 cm), the concentration of inorganic nitrogen increases (Lin et al., 2014), suggesting that

remineralization of organic compounds is the major pathway where the decay process is accompanied by conversion of organic N to NH_3. Soil microorganisms utilize part of this inorganic N for synthesis of new cells. Moreover, some of the ammonia formed might be used to produce low molecular weight stable nitrogen complexes. Interestingly, most of the changes that were detected were in the organic nitrogen compounds that fell in the lignin-like region of the van Krevelen diagram and not the amino acids region. This might be the case since amino acid turnover in soils is very rapid, half-lives may be as long as 20 h in soils with no plants, but they are usually less than 3 h and may be less than 1 h (Jämtgård et al., 2008; Jones & Darrah, 1994; Schobert & Komor, 1987).

4.3.3. S,N-Containing Compounds

The abundance of unique CHONS compounds mainly at the intermediate depth zone is a very interesting observation (Figures 6c and 7). CHONS compounds at the S1 bog exist in two different forms (1) as polycyclic aromatic compounds (PAC) characterized by low O/C and H/C ratios that contain two heteroatoms and (2) as lignin-like compounds characterized by intermediate H/C and O/C ratios. The presence of PAC compounds that contain two heteroatoms in peatland pore water DOM has never been reported. Nishioka and Lee (1987) reported the presence of polycyclic aromatic compounds containing both sulfur and nitrogen in coal-derived products in a solvent-refined coal liquid and a coal tar using gas chromatography-mass spectrometry. Even though peat is the starting material for coal formation, coal is only formed when peat is altered physically, chemically, and biologically. The source of these compounds and their fate are not yet known.

PAC compounds are also known as priority pollutants that could be formed through anthropogenic pyrolitic process and ubiquitously distributed in the environment (Grimalt et al., 2004; Laflamme & Hites, 1978) Considering that the Marcell Experimental Forest site location far from direct industrial pollution, we think it is safe to rule out the possibility of pollution at this site. Interestingly, several investigations have pointed out that biological processes may also yield PACs. Blummer (1961) first reported that PACs occur as common constituents in soils from nonindustrial areas. Later Graf and Diehl (1966) reported PAC formation associated with plant metabolism. Recently, Thiele et al. (2002) hypothesized that PACs not only are residually accumulated through biological activities but also are formed via enzymatic reactions in oxygen deficient soils. The concentrations of these compounds decreased during incubation (Thiele et al., 2002). The decrease was attributed due to anaerobic degradation, suggesting that these compounds could also be bioavailable after formation. Wilcke et al. (2000) presented strong indications for large biological sources of PACs in the Amazonian Basin. While the actual mechanism of how PAC compounds are formed in peat is not clear, possibilities include the isoprene metabolic pathway, cyclization of amino acids, alkylation, rearrangement, and oxidation. In this system, it is believed that the intense decomposition occurring at the intermediate depth zone results in the formation of precursor material that undergoes alkylation, cyclization, and rearrangement reactions to produce PACs. The presence of N and S compounds at the intermediate depth will favor the formation of PAC with heteroatoms. Below the intermediate depth, these compounds likely undergo degradation and hydrogenation reactions to produce compounds with higher H:C ratios. Alternatively, fire could be another source of these compounds. Recently, a microscopic image of peat from the middepth zone revealed some features that could indicate black carbon presence (Figure S4).

5. Conclusions

Consistent with our hypotheses, pore water organic compounds showed strong vertical stratification that could be categorized into three depth zones. Surface samples (<25 cm) were dominated by inputs from vegetation, while the intermediate depth zone (~ 50 cm) was an area of high reactivity with digenetic formation of many new unique compounds, including those with heteroatoms. We believe the higher evidence of carbon, sulfur, and nitrogen turn over at the intermediate depth zones is associated with redox oscillations due to fluctuating water table depth across the seasons. At these intermediate depths, high MW compounds were formed that were then preferentially decomposed in the deeper layers (>75 cm) where newly formed recalcitrant compounds accumulated. Below 75 cm fewer unique compounds were observed, and DOM became more lignin-like, more similar to surface samples but with less lipid-like compounds.

Pore water flow though the deep anaerobic portion of the peat column, the catotelm, has been considered negligible (Clymo, 1984), and the input of organic matter to the catotelm was assumed to occur only at its surface, the bottom of the acrotelm. The importance of DOM downward advection to the deeper

peat was not appreciated, and microbial respiration was thought to be feeding on peat itself only. Siegel et al. (1995) however showed that bogs could be hydraulically active with components of both vertical and lateral flow. Chanton et al. (1995) and Chanton et al. (2008) showed that advection could supply DOM to fuel microbial respiration in the catotelm. Our detailed characterization of DOM composition and EEM-PARAFAC was consistent with similar radiocarbon evidence presented in Tfaily et al. (2014) and Wilson et al. (2016) that showed transport of DOM and evidence of its utilization by microbial communities at depth in the S1 bog.

Surface and deep DOM exhibited relatively similar characteristics, with the deep layer having a higher input of microbially degraded organic matter than the surface suggesting that the entire peat profile consisted of similar parent material at different degrees of decomposition and that lateral and vertical advection of pore water from the surface to the deeper horizons is responsible for such similarities. However, the intermediate depth profile experiences increased decomposition compared to the surface and deep horizons and thus the most diverse composition of DOM compounds. Our results highlight the importance of understanding processes that control DOM production and transformation with depth. Our findings suggest that molecular composition of DOM in peatland pore water is dynamic and is a function of ecosystem activity, water table depth, and redox oscillations.

Overall, our findings support our hypothesis that environmental factors such as redox oscillations increase the complexity of the molecular composition of DOM and microbial communities and are key controlling factors in the carbon cycle. Furthermore, biogeochemical processing of DOM in peatlands can alter its chemical quality and its bioavailability to the local microbiology. This study sheds new light on the molecular-scale mechanisms related to degradation and production of nitrogen- and sulfur-containing compounds, including polyaromatic hydrocarbons in peatland pore waters. Our results highlight the importance of understanding processes that control DOM production and transformation with depth.

Acknowledgments
We thank Randall Kolka, MN forest services, and the rest of SPRUCE team for their help with sample handling and providing laboratory space support. This work was supported by the Office of Biological and Environmental Research, Terrestrial Ecosystem Science Program, under U.S. DOE contract ER65245. The SPRUCE experiment is supported by the United States Department of Energy, Office of Science, Biological and Environmental Research under contract DE-AC05-00OR22725. Oak Ridge National Laboratory is managed by UT-Battelle, LLC for the United States Department of Energy. Mass spectra were obtained at the National High Magnetic Field Laboratory FT-ICR Facility in Tallahassee, FL (Project NSF DMR-1157490). A portion of this work was also done at EMSL, a DOE Office of Science User Facility sponsored by BER and located at Pacific Northwest National Laboratory (PNNL). PNNL is operated by Battelle for DOE. https://doi.org/10.5281/zenodo.816210; https://doi.org/10.5281/zenodo.816210.

References

Akagi, J., & Zsolnay, A. (2008). Effects of long-term de-vegetation on the quantity and quality of water extractable organic matter (WEOM): Biogeochemical implications. *Chemosphere*, *72*, 1462–1466. https://doi.org/10.1016/j.chemosphere.2008.05.009

Andersson, C. A., & Bro, R. (2000). The N-way Toolbox for MATLAB. *Chemometrics and Intelligent Laboratory Systems*, *52*(1), 1–4. https://doi.org/10.1016/S0169-7439(00)00071-X

Armstrong, W., Cousins, D., Armstrong, J., Turner, D. W., & Beckett, P. M. (2000). Oxygen distribution in wetland plant roots and permeability barriers to gas-exchange with the rhizosphere: A microelectrode and modelling study with *Phragmites australis*. *Annals of Botany-London*, *86*(3), 687–703. https://doi.org/10.1006/anbo.2000.1236

Blodau, C., Roulet, N. T., Heitmann, T., Stewart, H., Beer, J., Lafleur, P., & Moore, T. R. (2007). Belowground carbon turnover in a temperate ombrotrophic bog. *Global Biogeochemical Cycles*, *21*, GB1021. https://doi.org/10.1029/2005GB002659

Blummer, M. (1961). Benzopyrenes in soils. *Science*, *134*, 474–475.

Chanton, J. E., Bauer, J., Glaser, E., Siegel, D., Ramonowitz, E., Tyler, S., et al. (1995). Radiocarbon evidence for the substrates supporting methane formation within northern Minnesota peatlands. *Geochimica et Cosmochimica Acta*, *59*, 3663–3668.

Chanton, J. P., Glaser, P. H., Chasar, L. S., Burdige, D. J., Hines, M. E., Siegel, D. I., et al. (2008). Radiocarbon evidence for the importance of surface vegetation on fermentation and methanogenesis in contrasting types of boreal peatlands. *Global Biogeochemical Cycles*, *22*, GB4022. https://doi.org/10.1029/2008GB003274

Chowdhury, S. K., Katta, V., & Chait, B. T. (1990). Electrospray ionization mass-spectrometric peptide-mapping—A rapid, sensitive technique for protein-structure analysis. *Biochemical and Biophysical Research Communications*, *167*(2), 686–692. https://doi.org/10.1016/0006-291x(90)92080-J

Clymo, R. S. (1984). The limits to peat bog growth. *Philosophical Transactions of the Royal Society B*, *303*, 605–654.

Clymo, R. S., & Bryant, C. L. (2008). Diffusion and mass flow of dissolved carbon dioxide, methane, and dissolved organic carbon in a 7-m deep raised peat bog. *Geochimica et Cosmochimica Acta*, *72*, 2048–2066. https://doi.org/10.1016/j.gca.2008.01.032

Corbett, J. E., Burdige, D. J., Tfaily, M. M., Dial, A. R., Cooper, W. T., Glaser, P. H., & Chanton, J. P. (2013). Surface production fuels deep heterotrophic respiration in northern peatlands. *Global Biogeochemical Cycles*, *27*, 1163–1174. https://doi.org/10.1002/2013GB004677

Corbett, J. E., Tfaily, M. M., Burdige, D. J., Cooper, W. T., Glaser, P. H., & Chanton, J. P. (2013). Partitioning pathways of CO_2 production in peatlands with stable carbon isotopes. *Biogeochemistry*, *114*(1), 327–340. https://doi.org/10.1007/s10533-012-9813-1

Corbett, J. E., Tfaily, M. M., Burdige, D. J., Glaser, P. H., & Chanton, J. P. (2015). The relative importance of methanogenesis in the decomposition of organic matter in northern peatlands. *Journal of Geophysical Research: Biogeosciences*, *120*, 280–293. https://doi.org/10.1002/2014JG002797

Dise, N. B. (2009). Peatland response to global change. *Science*, *326*(5954), 810–811. https://doi.org/10.1126/science.1174268

Findlay, S., Quinn, J. M., Hickey, C. W., Burrell, G., & Downes, M. (2001). Effects of land use and riparian flowpath on delivery of dissolved organic carbon to streams. *Limnology and Oceanography*, *46*(2), 345–355.

Freeman, C., Fenner, N., Ostle, N. J., Kang, H., Dowrick, D. J., Reynolds, B., et al. (2004). Export of dissolved organic carbon from peatlands under elevated carbon dioxide levels. *Nature*, *430*, 195–198. https://doi.org/10.1038/nature02707

Frolking, S., Talbot, J., Jones, M. C., Treat, C. C., Kauffman, J. B., Tuittila, E. S., & Roulet, N. (2011). Peatlands in the Earth's 21st century climate system. *Environmental Reviews*, *19*, 371–396. https://doi.org/10.1139/A11-014

Gorham, E. (1991). Northern peatlands—Role in the carbon-cycle and probable responses to climatic warming. *Ecological Applications*, *1*(2), 182–195. https://doi.org/10.2307/1941811

Graf, W., & Diehl, H. (1966). Uber Den Naturbedingten Normalpegel Kanzerogener Polycyclischer Aromate Und Seine Ursache. *Archiv für Hygiene und Bakteriologie*, *150*(1-2), 49.

Griffiths, N. A., & Sebestyen, S. D. (2016). Dynamic vertical profiles of peat porewater chemistry in a northern peatland. *Wetlands*, *36*, 1119–1130.

Grimalt, J. O., van Drooge, B. L., Ribes, A., Fernandez, P., & Appleby, P. (2004). Polycyclic aromatic hydrocarbon composition in soils and sediments of high altitude lakes. *Environmental Pollution*, *131*, 13–24. https://doi.org/10.1016/j.envpol.2004.02.024

Hanson, P. J., Gill, A. L., Xu, X., Phillips, J. R., Weston, D. J., Kolka, R. K., et al. (2016). Intermediate-scale community-level flux of CO2 and CH4 in a Minnesota peatland: putting the SPRUCE project in a global context. *Biogeochemistry*, *129*, 255–272.

Holden, J. (2005). Peatland hydrology and carbon release: Why small-scale process matters. *Philosophical Transactions of the Royal Society A*, *363*, 2891–2913. https://doi.org/10.1098/rsta.2005.1671

Huryn, A. D., Riley, R. H., Young, R. G., Arbuckle, C. J., Peacock, K., & Lyon, G. (2001). Temporal shift in contribution of terrestrial organic matter to consumer production in a grassland river. *Freshwater Biology*, *46*(2), 213–226. https://doi.org/10.1046/j.1365-2427.2001.00648.x

Jämtgård, S., Näsholm, T., & Huss-Danell, K. (2008). Characteristics of amino acid uptake in barley. *Plant and Soil*, *302*, 221–231. https://doi.org/10.1007/s11104-007-9473-4

Jones, D. L., & Darrah, P. R. (1994). Amino-acid influx at the soil-root interface of *Zea mays* L and its implications in the rhizosphere. *Plant and Soil*, *163*(1), 1–12.

Kolka, R. (2011). *Peatland Biogeochemistry and Watershed Hydrology at the Marcell Experimental Forest* (Vol. xxiv, 488 pp.). Boca Raton: CRC Press.

Laflamme, R. E., & Hites, R. A. (1978). The global distribution of polycyclic aromatic hydrocarbons in recent sediments. *Geochimica et Cosmochimica Acta*, *42*(3), 289–303. https://doi.org/10.1016/0016-7037(78)90182-5

Limpens, J., Berendse, F., Blodau, C., Canadell, J. G., Freeman, C., Holden, J., et al. (2008). Peatlands and the carbon cycle: From local processes to global implications a synthesis (vol 5, pg 1475, 2008). *Biogeosciences*, *5*(6), 1739–1739.

Lin, X. J., Tfaily, M. M., Steinweg, M., Chanton, P., Esson, K., Yang, Z. K., et al. (2014). Microbial community stratification linked to utilization of carbohydrates and phosphorus limitation in a boreal peatland at Marcell Experimental Forest, Minnesota, USA. *Applied and Environmental Microbiology*, *80*(11), 3518–3530. https://doi.org/10.1128/Aem.00205-14

Lin, X., Tfaily, M. M., Green, S. J., Steinweg, J. M., Chanton, P., Imvittaya, A., et al. (2014). Microbial metabolic potential for carbon degradation and nutrient (nitrogen and phosphorus) acquisition in an ombrotrophic peatland. *Applied and Environmental Microbiology*, *80*(11), 3531–3540. https://doi.org/10.1128/Aem.00206-14

Lovley, D. R., & Klug, M. J. (1986). Model for the distribution of sulfate reduction and methanogenesis in freshwater sediments. *Geochimica et Cosmochimica Acta*, *50*(1), 11–18. https://doi.org/10.1016/0016-7037(86)90043-8

Nichols, D. S., & Brown, J. M. (1980). Evaporation from a sphagnum moss surface. *Journal of Hydrology*, *48*(3-4), 289–302. https://doi.org/10.1016/0022-1694(80)90121-3

Nishioka, M., & Lee, M. L. (1987). Preferred annellated structures of polycyclic aromatic compounds in coal-derived materials. In *Polynuclear Aromatic Compounds* (pp. 235–253). Washington, DC: American Chemical Society. https://doi.org/10.1021/ba-1988-0217.ch01410.1021/ba-1988-0217.ch014

Novak, M., Kirchner, J. W., Groscheova, H., Havel, M., Cerny, J., Krejci, R., & Buzek, F. (2000). Sulfur isotope dynamics in two central European watersheds affected by high atmospheric deposition of SO_x. *Geochimica et Cosmochimica Acta*, *64*(3), 367–383. https://doi.org/10.1016/S0016-7037(99)00298-7

Ohno, T., & Bro, R. (2006). Dissolved organic matter characterization using multiway spectral decomposition of fluorescence landscapes. *Soil Science Society of America Journal*, *70*, 2028–2037. https://doi.org/10.2136/sssaj2006.0005

Parmesan, C., & Hanley, M. E. (2015). Plants and climate change: Complexities and surprises. *Annals of Botany-London*, *116*(6), 849–864. https://doi.org/10.1093/aob/mcv169

Parsekian, A. D., Slater, L., & Giménez, D. (2012). Application of ground-penetrating radar to measure near-saturation soil water content in peat soils. *Water Resources Research*, *48*, W02533. https://doi.org/10.1029/2011WR011303

Pendall, E., et al. (2004). Below-ground process responses to elevated CO_2 and temperature: A discussion of observations, measurement methods, and models. *The New Phytologist*, *162*(2), 311–322. https://doi.org/10.1111/j.1469-8137.2004.01053.x

Riley, R. H., Townsend, C. R., Niyogi, D. K., Arbuckle, C. A., & Peacock, K. A. (2003). Headwater stream response to grassland agricultural development in New Zealand. *New Zealand Journal of Marine and Freshwater*, *37*(2), 389–403.

Schobert, C., & Komor, E. (1987). Amino-acid-uptake by *Ricinus communis* roots—Characterization and physiological significance. *Plant, Cell & Environment*, *10*(6), 493–500. https://doi.org/10.1111/j.1365-3040.1987.tb01827.x

Sebestyen, S. D., Dorrance, C., Olson, D., Verry, E. S., Kolka, R. K., Elling, A. E., & Kyllander, R. (2011). Long-term monitoring sites and trends at the Marcell Experimental Forest. In R. K. Kolka, S. D. Sebestyen, E. S. Verry, & K. N. Brooks (Eds.), *Peatland Biogeochemistry and Watershed Hydrology at the Marcell Experimental Forest* (pp. 15–71). Boca Raton, FL: CRC press.

Senesi, N. (1990). Molecular and quantitative aspects of the chemistry of fulvic-acid and its interactions with metal-ions and organic-chemicals 2. The fluorescence spectroscopy approach. *Analytica Chimica Acta*, *232*(1), 77–106. https://doi.org/10.1016/S0003-2670(00)81226-X

Siegel, D. I., & Glaser, P. H. (1987). Groundwater-flow in a bog fen complex, lost river peatland, northern Minnesota. *Journal of Ecology*, *75*(3), 743–754. https://doi.org/10.2307/2260203

Siegel, D. I., Reeve, A. S., Glaser, P. H., & Romanowicz, E. A. (1995). Climate-driven flushing of pore water in peatlands. *Nature*, *374*(6522), 531–533.

Stedmon, C. A., & Bro, R. (2008). Characterizing dissolved organic matter fluorescence with parallel factor analysis: A tutorial. *Limnology and Oceanography: Methods*, *6*, 572–579.

Stedmon, C. A., Markager, S., & Bro, R. (2003). Tracing dissolved organic matter in aquatic environments using a new approach to fluorescence spectroscopy. *Marine Chemistry*, *82*(3-4), 239–254. https://doi.org/10.1016/S0304-4203(03)00072-0

Tfaily, M. M., Podgorski, D. C., Corbett, J. E., Chanton, J. P., & Cooper, W. T. (2011). Influence of acidification on the optical properties and molecular composition of dissolved organic matter. *Analytica Chimica Acta*, *706*(2), 261–267.

Tfaily, M. M., Hodgkins, S., Podgorski, D. C., Chanton, J. P., & Cooper, W. T. (2012). Comparison of dialysis and solid-phase extraction for isolation and concentration of dissolved organic matter prior to Fourier transform ion cyclotron resonance mass spectrometry. *Analytical and Bioanalytical Chemistry*, *404*, 447–457. https://doi.org/10.1007/s00216-012-6120-6

Tfaily, M. M., Hamdan, R., Corbett, J. E., Chanton, J. P., Glaser, P. H., & Cooper, W. T. (2013). Investigating dissolved organic matter decomposition in northern peatlands using complimentary analytical techniques. *Geochimica et Cosmochimica Acta*, *112*, 116–129.

Tfaily, M. M., Cooper, W. T., Kostka, J. E., Chanton, P. R., Schadt, C. W., Hanson, P. J., et al. (2014). Organic matter transformation in the peat column at Marcell Experimental Forest: Humification and vertical stratification. *Journal of Geophysical Research: Biogeosciences*, *119*, 661–675. https://doi.org/10.1002/2013JG002492

Tfaily, M. M., Corbett, J. E., Wilson, R., Chanton, J. P., Glaser, P. H., Cawley, K. M., et al. (2015). Utilization of PARAFAC-modeled excitation-emission matrix (EEM) fluorescence spectroscopy to identify biogeochemical processing of dissolved organic matter in a northern peatland. *Photochemistry and Photobiology*, *91*(3), 684–695. https://doi.org/10.1111/php.12448

Thiele, S., Fernandes, E., & Bollag, J. M. (2002). Enzymatic transformation and binding of labeled 2,4,6-trinitrotoluene to humic substances during an anaerobic/aerobic incubation. *Journal of Environmental Quality*, *31*(2), 437–444.

Urban, N. R., Eisenreich, S. J., & Grigal, D. F. (1989). Sulfur cycling in a forested sphagnum bog in northern Minnesota. *Biogeochemistry*, *7*(2), 81–109. https://doi.org/10.1007/Bf00004123

Vanbreemen, N. (1995). Nutrient cycling strategies. *Plant and Soil*, *168*, 321–326.

Verry, E. S. (1981). Water table and streamflow changes after stripcutting and clearcutting an undrained black spruce bog. In *Proceedings of the Sixth International Peat Congress, Duluth, MN, August 17-23, 1980* (pp. 493–498). International Peat Society: Eveleth, MN.

Wilcke, W., Amelung, W., Martius, C., Garcia, M. V. B., & Zech, W. (2000). Biological sources of polycyclic aromatic hydrocarbons (PAHs) in the Amazonian rain forest. *Journal of Plant Nutrition and Soil Science*, *163*(1), 27–30.

Wilson, R. M., Hopple, A. M., Tfaily, M. M., Sebestyen, S. D., Schadt, C. W., Pfeifer-Meister, L., et al. (2016). Stability of peatland carbon to rising temperatures. *Nature Communications*, *7*, 13,723.